

A hydrogeological landscape framework to identify peatland wildfire smouldering hotspots

Hokanson, Kelly Jean; Moore, Paul A.; Lukenbach, Max; Devito, Kevin J.; Kettridge, Nicholas; Petrone, Rich; Mendoza, Carl; Waddington, James Michael

DOI:
[10.1002/eco.1942](https://doi.org/10.1002/eco.1942)

License:
None: All rights reserved

Document Version
Peer reviewed version

Citation for published version (Harvard):
Hokanson, KJ, Moore, PA, Lukenbach, M, Devito, KJ, Kettridge, N, Petrone, R, Mendoza, C & Waddington, JM 2018, 'A hydrogeological landscape framework to identify peatland wildfire smouldering hotspots', *Ecohydrology*, vol. 11, no. 4, e1942. <https://doi.org/10.1002/eco.1942>

[Link to publication on Research at Birmingham portal](#)

Publisher Rights Statement:

This is the peer reviewed version of the following article: Hokanson, K. J., et al. "A HYDROGEOLOGICAL LANDSCAPE FRAMEWORK TO IDENTIFY PEATLAND WILDFIRE SMOULDERING HOTSPOTS." *Ecohydrology*, which has been published in final form at: <http://dx.doi.org/10.1002/eco.1942>. This article may be used for non-commercial purposes in accordance with Wiley Terms and Conditions for Self-Archiving.

General rights

Unless a licence is specified above, all rights (including copyright and moral rights) in this document are retained by the authors and/or the copyright holders. The express permission of the copyright holder must be obtained for any use of this material other than for purposes permitted by law.

- Users may freely distribute the URL that is used to identify this publication.
- Users may download and/or print one copy of the publication from the University of Birmingham research portal for the purpose of private study or non-commercial research.
- User may use extracts from the document in line with the concept of 'fair dealing' under the Copyright, Designs and Patents Act 1988 (?)
- Users may not further distribute the material nor use it for the purposes of commercial gain.

Where a licence is displayed above, please note the terms and conditions of the licence govern your use of this document.

When citing, please reference the published version.

Take down policy

While the University of Birmingham exercises care and attention in making items available there are rare occasions when an item has been uploaded in error or has been deemed to be commercially or otherwise sensitive.

If you believe that this is the case for this document, please contact UBIRA@lists.bham.ac.uk providing details and we will remove access to the work immediately and investigate.

1 **A HYDROGEOLOGICAL LANDSCAPE FRAMEWORK**
2 **TO IDENTIFY PEATLAND WILDFIRE SMOULDERING HOTSPOTS**

3
4 **K.J. HOKANSON^{1,2,3*}, P.A. MOORE¹, M.C. LUKENBACH^{1,3}, K.J. DEVITO²,**
5 **N. KETTRIDGE⁴, R.M. PETRONE⁵, C.A. MENDOZA³, J.M. WADDINGTON¹**

6
7 ¹School of Geography and Earth Sciences, McMaster University, Hamilton, ON, L8S
8 4K1, Canada.

9 ²Department of Biological Sciences, University of Alberta, Edmonton, AB, T6G 2E9
10 Canada.

11 ³Department of Earth and Atmospheric Sciences, University of Alberta, Edmonton, AB,
12 T6G 2E3, Canada

13 ⁴School of Geography, Earth and Environmental Sciences, University of Birmingham,
14 Edgbaston, Birmingham, B15 2TT, UK.

15 ⁵Department of Geography and Environmental Management, University of Waterloo,
16 Waterloo, ON, N2L 3G1, Canada.

17
18 *Corresponding author: Kelly J Hokanson, email: hokanson@ualberta.ca

19
20 Keywords: peatland, wildfire, carbon, boreal, organic soil, hydrogeology,

21
22 Running Head: A hydrogeological framework to identify peatland smouldering hotspots

23
24

25 **ABSTRACT**

26 Northern peatlands are important global carbon stores, but there is concern these boreal
27 peat reserves are at risk due to increased fire frequency and severity as predicted by
28 climate change models. In a sub-humid climate, hydrogeological position is an important
29 control on peatland hydrology and wildfire vulnerability. Consequently, we hypothesized
30 that in a coarse-textured glaciofluvial outwash, isolated peatlands lacking the moderating
31 effect of large-scale groundwater flow would have greater water-table (WT) variability
32 and would also be more vulnerable to deep WT drawdown and wildfire during dry
33 climate cycles. A holistic approach was taken to evaluate three well accepted factors that
34 are associated with smouldering in boreal peatlands: hollow microform coverage,
35 peatland margin morphometry, and gravimetric water content. Using a combination of
36 field measurements (bulk density, humification, WT position, hummock-hollow
37 distribution, and margin width) and modelling (1-D vertical unsaturated flow coupled
38 with a simple peat-fuel energy balance equation) we assessed the vulnerability of peat to
39 smouldering. We found that a peatland in the regionally intermediate topographic
40 position is the most vulnerable to smouldering due to the interaction of variable
41 connectivity to large-scale groundwater flow and the absence of mineral stratigraphy for
42 limiting WT declines during dry conditions. Our findings represent a novel assessment
43 framework and tool for fire managers by providing *a priori* knowledge of potential peat
44 smouldering hotspot locations in the landscape to efficiently allocate resources and
45 reduce emergency response time to smouldering events.

INTRODUCTION

Peatland ecosystems cover 25 – 30% of boreal regions and represent a long-term sink of atmospheric CO₂, storing ~ 220 – 550 Pg C (Yu, 2011). Wildfire is the largest disturbance affecting these ecosystems, accounting for >97% of all disturbances (by area) (Turetsky *et al.*, 2002). While peatlands are generally resilient to wildfire disturbance (Thompson and Waddington, 2013), northern peat fires can emit considerable amounts of CO₂ (*e.g.*, Turetsky *et al.*, 2002) and harmful smoke pollution (Shaposhinkov *et al.*, 2014). Moreover, because the size of large (> 140,000 ha) wildfires has been shown to increase positively with peatland abundance (Turetsky *et al.*, 2004), northern peat fires also represent a challenging and costly fire management issue. These smouldering peat fires are especially challenging in sub-humid boreal regions, such as Western Canada, where the fire return interval is less than 100–120 years (Turetsky *et al.*, 2004) and the propensity for drier peat is common (Waddington *et al.*, 2015). Moreover, there is concern that peat burn severity and associated wildfire management costs will increase due to warmer and drier conditions with climate change (Turetsky *et al.*, 2004). As such, there is an urgent and growing need to identify potential hotspots for peat smouldering on the landscape to increase the efficacy of wildfire management and mitigation strategies. Here we present a landscape framework that combines moss ecohydrology, peatland hydrology, and regional hydrogeology to identify potential peat-smouldering hotspots in the Utikuma region of Alberta's Boreal Plains (BP) where peat fires are common (*e.g.*, Benscoter *et al.*, 2015; Lukenbach *et al.*, 2015).

Our hydrogeological landscape approach provides a framework for current and future research in this region, which has demonstrated that peat burn severity is higher in peat

70 profiles with low gravimetric water contents (GWC) (Rein *et al.*, 2008) and/or high peat
71 dry bulk density (ρ_b) (Benscoter *et al.*, 2011) and is a function of: i) *Sphagnum fuscum*
72 (*Schimp.*) *H.Klinggr.* hummock cover (*e.g.*, Benscoter *et al.*, 2015), ii) peatland margin
73 cover (Lukenbach *et al.*, 2015) and iii) groundwater connectivity (Hokanson *et al.*, 2016).
74 Briefly, *S. fuscum* hummocks, which have high water retention and low ρ_b , often
75 experience low burn severity, and in many cases are resistant to ignition (Benscoter *et al.*,
76 2011). In the BP, margin peat is often denser and drier than peat in the central portion of
77 the peatland due to more persistently low and/or fluctuating water-tables (see Lukenbach
78 *et al.*, 2015 for details). Hokanson *et al.* (2016) also identified that peatlands with high
79 groundwater connectivity had low burn severity owing to persistently higher GWC.
80 Furthermore, Devito *et al.* (2012) illustrated the type of mineral sediment and relation to
81 regional water-tables considerably influence location and connectedness of peatlands.
82 Without the moderating effect of regional groundwater flow, isolated peatlands have
83 greater WT variability, and are more vulnerable to deep WT drawdown during dry
84 climate cycles. As such, the topographic position of a peatland in a coarse-textured HRA
85 plays a large role in determining the hydrophysical properties of margin peat and the
86 distribution of *S. fuscum* hummocks and therefore its vulnerability to combustion
87 (Hokanson *et al.*, 2016).

88
89 To assess our hydrogeological landscape framework we examined a large topographic
90 gradient, ranging from a low-lying flow-through peatland (*i.e.*, high groundwater
91 connectivity) to a completely perched peatland (*i.e.*, no groundwater connectivity), and
92 examined the primary hydrophysical controls on peatland burn severity and carbon loss:
93 *S.fuscum* hummock cover, peatland margin cover, ρ_b , and GWC. We hypothesized that

the potential for smouldering hotspots would increase with decreasing connection from groundwater due to a decrease in higher WT buffering, an increase in percent margin cover and a decrease in the percent cover of *S.fuscum* hummocks. That is, low lying flow-through peatlands would be least vulnerable to deep smouldering due to higher WT buffering from a strong connection to the regional groundwater flow, with increasing vulnerability as the spatio-temporal connection to regional groundwater decreases.

METHODS

Study sites

This study was located at the Utikuma Region Study Area (URSA) located 370 km north of Edmonton, Alberta in the BP region of western Canada (Devito *et al.*, 2016). Annual potential ET often exceeds annual precipitation (517 mm and 481 mm respectively; Bothe and Abraham, 1993). Three URSA peatlands (Figure 1) were selected along a topographic gradient in the coarse-textured HRA (Figure 2d). Using historical (2003 – 2014) hydrological data (Smerdon *et al.*, 2005; Devito, *et al.*, 2016; Lukenbach *et al.*, 2017) each site is described below.

A low-lying flow-through kettle-hole peatland (site FT) is located on a regional topographic low in the URSA lake 208 catchment (Figure 1). Site FT is 0.8 ha and intersects a large-scale groundwater flow system connecting several ~450-900 ha lakes (Figure 1). These large groundwater-fed lakes moderate the water-table position in FT, minimizing extreme water-table fluctuations at the peatland margin and middle during periods of drought. Water-table fluctuations at FT range from 0.21 m below to 0.02 m

above the peat surface in the middle of the peatland, while margin water-table positions range from 0.32 m below to level with the peat surface (Table 1; Figure 2a).

A 0.68 ha peatland occupies an intermediate topographic position located in the URSA lake 16 catchment (Figure 1) and is ephemerally perched (site EP) due to transient connection to the regional water table. Site EP is located slightly above (~2.6 m) a regional groundwater flow system composed of a 'staircase' of lakes with an average horizontal gradient of 0.002 m m^{-1} (Smerdon *et al.*, 2005). The WT in the middle of the peatland ranges from 0.43 m to 0.93 m below the peat surface, while the margin experiences similar to greater long-term fluctuations, ranging from 0.45 m to 0.88 m below the surface (Figure 2b).

The peatland in the highest topographic position is a 1.56 ha perched peatland (site P) located in URSA lake 19 catchment (Figure 1). Site P has a laterally unconfined WT, confined vertically by layers of low permeability substrates overlying unsaturated coarse-textured sediments approximately 12 m above the regional WT. As such, P receives water solely from atmospheric inputs and has no connection to regional flow systems. The margin at P experiences large water-table fluctuations over time, ranging from 0.75 m below to 0.005 m above the peat surface (Table 1; Figure 2c) while the middle of P experiences minimal water-table fluctuations, ranging from 0.41 m below to level with the peat surface (Table 1; Figure 2c).

Study approach

We mapped the coverage of margins and hummocks at each of the peatlands and undertook detailed transects to determine the peat properties at the margin and middle of each peatland. Using peat water retention data from previous work (Moore et al., 2015), we parameterize the Peat Smouldering and Ignition model (PSI) (see Thompson *et al.*, 2015; Lukenbach *et al.*, 2015) to evaluate smouldering potential at each site. Details of the research design and methods are presented below.

Peatland mapping

The margin zone at each site was classified using lack of peatland microtopography as an indicator of transitional plant community (see Lukenbach *et al.*, 2015) and mapped to determine the percent margin cover. The relative cover of hummocks and hollows at each site was determined by establishing two perpendicular 50 m transects in the middle of each peatland. At one meter intervals, hummock-hollow microtopography was identified 1 m on either side of each transect (*i.e.*, 200 measurements per site). Peatland perimeter length was measured using DGPS points at roughly 2 m intervals. The peatland perimeter was defined by the location of a rapid transition in surface-ground cover from moss to bare soil and leaf litter, and lack of peat moss in the upper soil profile.

Peat properties

A 20 m transect was established at each site perpendicular to the peatland margin extending from the outer edge of the peatland towards the middle of the peatland. Every 2 m we described the presence or absence and type of surface peatland microform (hummock/hollow), measured organic soil depth (by coring), and determined vertical profiles of peat humification at 0.05 m intervals from the surface to mineral soil. The

degree of humification was determined using the von Post (VP) method (von Post and Granlund, 1926), which uses a categorical scale, from 1-10.

Peat cores (cross-sectional dimensions of 0.05 m x 0.05 m, depth 0.52 m) were extracted from both the margin and middle (hollow microforms only) of each peatland using a box corer to determine ρ_b (see Table 2 for sample sizes). Each monolith was sub-sampled vertically in the field at 0.04 m intervals using a serrated blade, and subsequently transported to a lab for analysis using standard methods. Peat humification was also determined on a random subset of monolith samples in order to develop a linear model for ρ_b using VP ($F_{8,621}=189.7$ $p<<0.01$; Adjusted R^2 : 0.706). Given the challenge and disturbance associated with extensive peat core extraction, this allowed us to estimate ρ_b for our simulated water content profiles at depths greater than 0.52 m.

Simulated peat water content profiles

Water content profiles were simulated by solving Richard's equation (Celia *et al.* 1990) for peat profiles with different specified pressure head (ψ) boundary conditions based on water-table depth (WTD). Both wet and dry scenarios were simulated for each site (FT, EP, and P), and location (margin and middle). Zero water pressure was specified for the lower boundary condition based on the upper and lower quartile (Table 1) of measured WTDs for each site-location combination. Initial ψ was set equal to the height above WT except for the surface boundary condition. The surface boundary ψ was calculated as a function of WTD as follows (adapted from Lukenbach et al., 2015):

$$\begin{aligned} \psi &= -(WTD + 0.02 \cdot (WTD - 0.4)) & WTD > 0.4 \text{ m} \\ \psi &= -WTD & WTD \leq 0.4 \text{ m} \end{aligned} \quad (1)$$

where ψ for WTD>0.4 m reflects typical measured disequilibrium conditions in the near surface. Steady-state ψ profiles were iteratively solved using the finite-difference discretization of the mixed form of Richard's equation (Celia *et al.* 1990). Simulations were evaluated using 0.04 m thick layers, where a steady-state condition was defined by a maximum change in ψ of 1×10^{-5} m. Layer properties for upper 0.52 m were based on measured ρ_b profiles for each site-location combination, where 100 profiles per site-location were generated by randomly sampling from layer-specific distributions using the mean and standard deviation of measured ρ_b (Table 2). A similar approach was used to simulate peat layers below 0.52 m depth, but where ρ_b was derived from the linear model relating VP to ρ_b (see *Peat properties*). Error estimates on the linear model coefficients were used to account for the variance in ρ_b associated with a given value of VP.

To parameterize saturated hydraulic conductivity (K_{sat}), we opted to use the ρ_b -dependent equation presented in Boelter (1969). Uncertainty associated with our parameterization of K_{sat} was not assessed in our analysis. Water retention and associated van Genuchten parameters were estimated from empirical relations between ψ , ρ_b , and water content as presented in Moore *et al.* (2015):

$$\frac{\theta_{\psi}}{\phi} = \frac{(a \cdot \ln \psi + b)^{-1} \cdot \rho_b}{\sqrt{1 + ((a \cdot \ln \psi + b)^{-1} \cdot \rho_b)^2}}$$

where θ_{ψ} is the volumetric water content at a specific ψ , ϕ is the porosity and a and b are fitted parameters. Empirical parameters were derived from water retention of peat samples from the URSA (Thompson and Waddington, 2013; Lukenbach *et al.*, 2015). To reduce the degrees of freedom, simulated profiles reflect water retention properties of hollow peat only, with corresponding a and b values of 38.3 ± 0.9 and 28.6 ± 7.2 , respectively.

208

209 *Peat Smouldering and Ignition model*

210 We parameterized the PSI model to assess peat smouldering propagation potential by
211 examining the ratio of the energy released by an overlying layer of peat (H_{comb}) to the
212 energy required to combust the layer of peat below (H_{ign}). H_{comb}/H_{ign} ratios < 1 have little
213 potential to smoulder because there is not enough available energy from the combustion
214 of the overlying layer to ignite the lower layer. The greater the H_{comb}/H_{ign} ratio the greater
215 the potential for downward smouldering to progress. The PSI model does not attempt to
216 model precise depths of burn, but has proven to be a useful approach to evaluating
217 peatland vulnerability at the landscape scale (*e.g.*, Lukenbach *et al.*, 2015).

218

219 *Statistical methods*

220 All statistical analyses were done using R (R Core Team, 2017). Linear model equations
221 in text are presented in Wilkinson notation. To test the significance of site, location (i.e.
222 middle, margin), and depth on measured ρ_b (i.e. samples taken to a maximum depth of
223 0.52 m), we used a linear mixed-effects model (LMM) (R-package *lme4*). Location and
224 depth were treated as fixed factors, and site as random. To test location as a factor, a
225 dummy variable was created where margin=0, and middle=1. Overall model significance
226 was assessed using analysis of variance (ANOVA) (R-function *anova*). Post-hoc tests
227 were done using the *lsmeans* function (R-package *lsmeans*), based on Tukey-adjusted
228 comparisons. A similar general linear model (GLM) approach was used for the simulated
229 peat water content and H_{comb}/H_{ign} ratios, where WT scenario was included as an
230 additional fixed factor, and site was treated as fixed as well. An ordinal logistic
231 regression (R-package MASS: *polr*) was used to analyze the effects of site, location (i.e.

distance from upland), and depth on VP. Due to the need to study peatlands with extensive historic hydrogeological data, only one peatland was studied in each topographic position. We therefore interpret our statistical analysis with caution due to the clear pseudo-replication. Specifically, we look for differences in site (*i.e.* FT, EP, P) rather than topographic position.

RESULTS

Peatland microtopography and morphometry

Hummocks were the dominant microform at FT, while hollow microforms dominated both EP and P (Table 1). The margin width ranged from 2 to 10 m (Table 1), where FT had the narrowest margin and EP had the widest. The EP site had a slightly higher perimeter-to-area ratio of 0.034 m m^{-2} compared to P and FT, with values of 0.028 and 0.025 m m^{-2} , respectively. Due to both a higher perimeter-to-area ratio and wide margin, EP had the greatest area classified as margin at 34%, compared 17% and 6% for FT and P, respectively (Table 1).

Peat properties

Both depth ($\text{Chi}^2=314.0$; $p<<0.01$) and location ($\text{Chi}^2=38.2$; $p<<0.01$) were found to be significant factors for explaining variance in ρ_b (H_1 : $\rho_b = \text{Location} + \text{Depth} + (1|\text{Site})$), when compared to the null model using just site as a random factor (H_0 : $\rho_b = 1 + (1|\text{Site})$). An ANOVA showed that nesting depth in location (H_2 : $\text{Location/Depth} + (1|\text{Site})$) did not significantly improve the model of ρ_b ($\text{Chi}^2=0.3554$; $p=0.551$) compared to H_1 , suggesting that the rate of change in ρ_b with depth is similar between middles and margins. The resulting linear model (H_1) is

$$\rho_b = 68 - 51 \cdot \text{location} + 356 \cdot \text{depth}$$

where ρ_b is in kg m^{-3} , and *depth* is in m (the random site intercepts are omitted). The post-hoc test (*lsmeans*) showed that measured ρ_b (Table 2) was significantly different between the middle and margin (z-ratio=11.8; $p < 0.01$) with a marginal mean difference of 51 kg m^{-3} (margin > middle). Similarly, the LMM shows that there was a relatively large increase in ρ_b with depth, at $356 \text{ kg m}^{-3} \text{ m}^{-1}$ based on measurements from the top 0.5 m of peat. Site differences in ρ_b account for 22% of overall variance, where all pairwise post-hoc tests show that ρ_b is significantly different between sites at a 0.05 significance level where $\text{FT} < \text{P} < \text{EP}$.

The humification profiles for FT (Figure 2a and 3) show that 98% of the first 0.4 m depth of the transect ranges from undecomposed ($\text{VP} = 1$) to slightly decomposed ($\text{VP} = 4$), which corresponds to an average ρ_b range of 26 to 112 kg m^{-3} . At EP and P, 44% and 66% of the top 0.4 m were at or below a VP of 4, respectively. VP was modelled using an ordinal logistic regression, where the average classification accuracy was 70% based k-fold cross validation. Regression results show that site, depth ($p < 0.01$), and the interaction of depth and distance along the transect ($p = 0.007$) had a significant effect on VP. While the odds ratio shows only a small likelihood of increasing VP with depth (1.03), this is on a per centimeter basis and thus becomes highly likely over the depth of a given peat profile. All else being equal, there is a significant likelihood of VP being lower at FT, and higher at EP compared to P, based on their respective odds ratios (FT=0.33; EP=1.86) (i.e $\text{FT} < \text{P} < \text{EP}$). Finally, while VP tends to increase with depth, the interaction term suggests that for a given depth, there is a small likelihood of decreasing

VP (odds ratio = 0.98) as you move from the peatland edge to interior. Again, it should be noted that the reported likelihood is based on a one meter change in lateral position.

Simulated peat water content profiles

Simulated volumetric water content (VWC) shows that VWC increases rapidly with depth when the WT is near the surface (e.g. FT), and much slower when WT is deep (e.g. EP) (Table 1 and Fig. 4a-c). A global analysis of the effect of depth, site, WT scenario, location (middle/margin) (Table 3) show that all main factors have significant effects on simulated VWC. Overall, site and depth have the largest effects on VWC, but several significant two- and three-way interactions exist (Table 3). GWC, which is VWC normalized by ρ_b , shows less consistent depth dependent patterns compared to VWC. Because there is a relatively large increase in ρ_b with depth (Table 2), GWC tends to decrease with depth when WT is deep (e.g. EP). The margin locations under the dry scenario at EP (median GWC of 221%) and P (median GWC of 235%) exhibited the lowest simulated GWC profiles, ranging from $350 \pm 91\%$ and $293 \pm 82\%$ (EP and P, respectively) at the surface to $166 \pm 78\%$ and $149 \pm 62\%$ at depth (Figure 4). EP showed significantly drier simulated GWC on a site-basis ($z\text{-ratio} \leq -7.11$, $p < 0.0001$), except compared to the margin at P ($z\text{-ratio} \geq -1.37$, $p \geq 0.75$). Site P was similar to the intermediate site, EP, at the margin location, but more similar to FT at the middle location.

Peat Smouldering and Ignition model

Broadly, simulated H_{comb}/H_{ign} ratios tended to be low at FT, high at EP, and more location-dependent (middle v. margin) at P. With a median value of 2.2 ± 0.8 , EP (dry,

margin) showed the highest H_{comb}/H_{ign} ratios, ranging from 1.1 ± 0.3 at the surface to 2.8 ± 0.6 at depth (Figure 5). Conversely, FT (wet, middle) showed the lowest H_{comb}/H_{ign} ratios, with a median value of 0.27 ± 0.4 , ranging from 0.7 ± 0.8 at the surface to 0.26 ± 0.02 at depth (Figure 4). A global analysis of the effect of depth, site, WT scenario, location, and their interactions (Table 3) show that all main factors have significant effects on simulated H_{comb}/H_{ign} ratios. There are several significant two- and three-way interactions. Focusing on the categorical variables, Fig. 6 shows that the only strong two-way interaction is between site and location. This is due to P, where H_{comb}/H_{ign} is high in the margin and low in the middle which contrasts with EP where H_{comb}/H_{ign} in the middle/margin is relatively high, while for FT H_{comb}/H_{ign} is generally low in both locations. While H_{comb}/H_{ign} is generally higher under the dry WT scenario, the interaction with site and location is similar to the wet WT scenario (Fig. 6) where the three-way interaction is not significant (Table 3).

DISCUSSION

Previous literature (*e.g.*, Benscoter *et al.* 2011, Lukenbach *et al.*, 2015) has approached peatland vulnerability from a peat properties perspective, focusing on profile-scale controls on peat-smouldering dynamics, such as GWC. Although a prior study (Hokanson *et al.*, 2016) observed differences in burn severity between landscape positions and peatland physiognomy (*i.e.*, percent hollow, percent margin, GWC), no prior studies have compared entire peatlands and evaluated them for overall vulnerability to intense peat smouldering. Our holistic approach, evaluating peatland vulnerability using microform coverage, margin morphometry, and GWC distribution, shows that in a coarse-textured hydrogeological landscape, peatlands at intermediate positions (EP) are

most susceptible to deep smouldering during a wildfire. While it was hypothesized that the perched peatland (P) would be most vulnerable due to its complete isolation from larger groundwater flow systems, it was actually shown that it was less vulnerable than a peatland with intermittent groundwater connection. The peatland that intersected a large groundwater flow system (FT) was, by far, the least vulnerable. The presence of large-scale groundwater flow at a low-lying peatland (FT) fostered higher percent hummock coverage, relatively small margin area, and high GWC under all WT scenarios, thereby limiting its vulnerability to smouldering. In contrast, a peatland perched above the regional WT receiving only atmospheric inputs, and a peatland ephemerally connected to larger scale groundwater flow exhibited comparatively lower hummock cover, higher relative margin area, and lower GWC values.

The prediction of relatively low GWC profiles and high H_{comb}/H_{ign} ratios strongly suggest that the peatland in the intermediate topographic position (EP) is the most vulnerable to deep smouldering. It has the highest incidence of predicted H_{comb}/H_{ign} ratios exceeding 1.0. While the margin at P has comparable H_{comb}/H_{ign} ratios under the dry scenario at some depths, it generally exhibited lower H_{comb}/H_{ign} ratios than the intermediate site, EP.

Peatland morphometry and physical properties

Site had a clear influence on microtopographic distributions and peatland margin cover, where a broader survey of peatlands across topographic position would be needed to determine whether spatio-temporal patterns of groundwater connection have a strong influence on peatland microtopography in coarse-textured HRAs. Nevertheless, we propose that FT had the highest hummock coverage (60%), likely due to the stable and high WT, while EP, the intermediate site, and P, the most isolated site, showed lower

hummock coverage (40% and 45%, respectively). Given that previous studies have shown that hummock microforms are resistant to burning during a wildfire, whereas hollow microforms are more prone to deep burning (Benscoter *et al.*, 2015; Lukenbach *et al.*, 2015), FT exhibits lower vulnerability to burning.

Contrary to our initial hypothesis, increasing isolation or disconnection from larger scale groundwater flow systems did not necessarily result in wider margins and greater margin cover. While the least isolated site, FT, had the lowest margin cover relative to P and EP, P had appreciably lower relative margin cover than EP. FT had, by far, the narrowest margin (2 m) resulting in a percentage of margin coverage of the total peatland of only 5.5%. Due to the strong influence of the large-scale groundwater flow system on the WT at FT, similar WT dynamics occurred at the middle and margin of the site, making the margin peat subject to similar moisture conditions as the middle. Additionally, the overarching effect of large-scale groundwater flow on the hydrology of the site appears to have minimized the distance (*i.e.*, margin width) to observe processes associated with margin development/formation, which may explain the rapid transition (*i.e.*, narrow margin) from the peatland to the mineral upland at the site. At EP and P, the magnitude of WT fluctuations was much more dramatic, corresponding with wider peatland margins, (10 and 6 meters respectively) and greater margin cover (34% and 17% respectively). While the absolute elevations of the WT do not vary significantly between the margin and the middle at EP, the WT does decline into the mineral soil below the margin (Figure 2b), leaving the margin peat hydraulically disconnected and free to decompose and densify (Waddington *et al.*, 2015). In contrast, surface and near-surface peat in the middle of the peatlands still maintain capillary connections with deeper

saturated peat during low WT conditions, limiting decomposition (Figure 2a-c). The WT depths at the margin of P were appreciably deeper than those in the middle of the peatland due to the perched nature of the peatland on a fine-textured lens in a coarse-textured landscape. Therefore, the WT drops precipitously, corresponding to a narrow margin compared to that of EP.

Simulated peat water content and Peat Smouldering and Ignition (PSI) model

At all three sites, ρ_b was shown to be systematically higher at the margins than in the middle of the peatlands. This supports the findings of previous work (Lukenbach *et al.*, 2015; Hokanson *et al.*, 2016). Bulk density accounts for the majority of the differences in GWC found between and within the sites (Figure 4), which compares well with previous studies (Benscoter *et al.*, 2011).

While some studies report GWC limits on smouldering as being between 93% and 145% (*e.g.*, Rein *et al.*, 2008), others report GWC limits ranging from 250% to 295%. Benscoter *et al.* (2011) observed smouldering of peat with GWC values of 295% and Davies *et al.* (2013) reported GWC values of over 252% in unburned reference cores while smouldering was occurring nearby in the same blanket bog. Furthermore, Benscoter *et al.* (2011) observed smouldering at depth at higher GWC limits than that required for surface ignition. Primarily, EP and P had GWC values fall within the range of previously reported values for smouldering peat. When both locations (middle, margin) and all associated depths are pooled, 54% of all simulated GWC values at EP under the dry scenario were <250%, while 41% of EP depths fell below 250% under the wet scenario. At P, 33% and 28% of depths fell below a GWC of 250% for dry and wet

scenarios, respectively. Only 3% of depths at FT under any scenario fell below a GWC of 250%, which is unlikely to sustain peat smouldering.

Expectedly, H_{comb}/H_{ign} ratios followed GWC and ρ_b trends closely at all sites, wherein low GWC values and high ρ_b values resulted in high H_{comb}/H_{ign} ratios. It is important to note that, while H_{comb}/H_{ign} ratios are a function of GWC, the results are not directly equivalent since H_{comb}/H_{ign} ratios take into account the effect of peat layering (*i.e.*, changes in ρ_b with depth). H_{comb}/H_{ign} ratios equaling 1 translates into a fuel profile whose heat of combustion exactly equals the heat required to both drive off the water and ignite the fuel in the underlying layer, assuming no heat is lost by mechanisms such as radiative or convective heat loss. Downward heat efficiencies reported by previous studies range from 0.3 to 0.9 with a mean of 0.7 (*e.g.*, Frandsen, 1998). A downward efficiency of 0.7 would require an H_{comb}/H_{ign} ratio of 1.4 for successful downward combustion between layers (Figure 5). The margins and middle at EP in the dry scenario meet this requirement at a majority of depths (76%). Site P, under dry conditions, only met this condition at 45% of depths, FT exhibited H_{comb}/H_{ign} ratios over 1.4 only 4% of the time.

von Post as a tool for rapid assessment of smouldering potential

Humification transects (Figure 3) show generally low levels of decomposition (*i.e.*, density) at FT and P, compared to that of EP. Using variability in peatland margin/middle VP to broadly infer ρ_b and water retention capacity, future studies could assess the landscape-scale importance of margin peat properties on vulnerability to smouldering across the BP. Using information on spatial and depth-dependence of VP in

BP peatlands could also be used to develop a high-level assessment of peat smouldering risk for wildfire managers.

Assessing peatland vulnerability to wildfire using a hydrogeological landscape approach

While it was originally hypothesized that as hydrologic connectivity decreased, vulnerability to smouldering would increase, we show that the completely perched (*i.e.* disconnected from regional groundwater) peatland (P) had a more moderated WT, and therefore a smaller relative margin area and lower ρ_b , than the intermediate site (EP). These peatlands are hydraulically mounded, resulting in deep WTs at the margins, which causes densification and drying of the peat (Waddington *et al.*, 2015). Site P has no connection with the regional WT, and one would expect it to be the most vulnerable to wildfire, especially in times of drought. However, the site conditions at P under maximum and minimum WT orientations are such that only a very narrow portion of the peatland is exposed during dry conditions (Figure 2). The severe WT decline at the margin is due to the sharp lithological transition of the silt and clay underlying the peatland to the sandy silt and fractured clay surrounding the peatland. While P is permanently perched well above the regional WT, intermediate sites (*e.g.*, EP) do not require such unique hydrostratigraphy, because they are transiently connected with the regional WT during wet climate cycles. This ephemeral connection could result in peat accumulation, and during dry climate conditions, result in drying and densification of margin peat as it becomes disconnected from the larger groundwater system.

CONCLUSION

We suggest that hydrogeological setting and topographic position are major controlling factors for deep smouldering hotspots in the BP. Low-lying flow-through peatlands that intersect the regional water table (FT) are the least vulnerable to deep smouldering, while peatlands in intermediate landscape positions (EP) are most vulnerable. Having *a priori* knowledge of potential smouldering hotspot locations in the landscape is beneficial for fire managers, allowing them to efficiently allocate resources and reduce emergency response time to smouldering events. While our goal was not to precisely model depths of burn, this approach is valuable for evaluating a peatland's relative vulnerability to deep smouldering and is a sound method of identifying wildfire vulnerability of peatland types within a particular HRA.

ACKNOWLEDGEMENTS

This research was funded by a Natural Sciences Engineering Research Council Discovery Grant to JMW and a research grant from Syncrude to KJD, NK, RMP and JMW, and Natural Sciences and Engineering Research Council-Collaborative Research and Development grant (NSERC-CRDPI477235-14) of Canada with industry partners Syncrude Canada Ltd and Canadian Natural Resources Limited. We thank Reyna Matties, Sarah Irvine and Cameron Irvine for assistance in the field and Carolynn Forsyth for camp facilities at Artis Inn. Lidar data were acquired by Airborne Imaging, Inc. and licensed to the Government of Alberta. The DEM was derived by Laura Chasmer by classifying ground and non-ground returns. We recognize and thank Todd Redding, Joe Riddell and countless others for their data collection efforts as part of the long-term URSA project. Finally, we thank Matt Davies and an anonymous reviewer.

467

468 **REFERENCES**

469 Benscoter, B.W., Greenacre, D., Turetsky, M.R. (2015). Wildfire as a key determinant of
470 peatland microtopography. *Canadian Journal of Forest Research*, **45**, 1132-1136, DOI:
471 10.1139/cjfr-2015-0028

472

473 Benscoter, B.W., Thompson, D.K., Waddington, J.M., Flannigan, M.D., Wotton, B.M.,
474 De Groot, W.J., Turetsky, M.R. (2011). Interactive effects of vegetation, soil moisture
475 and bulk density on depth of burning of thick organic soils. *International Journal of*
476 *Wildland Fire*, **20**, 418-429. DOI: 10.1071/WF08183.

477

478 Boelter, D.H. (1969). Physical properties of peats as related to degree of decomposition.
479 *Soil Science Society of America Journal*, **33**, 606-609.

480

481 Bothe, R.A. and Abraham, C. (1993). Evaporation and evapotranspiration in Alberta
482 1986 to 1992 addendum. Surface Water Assessment Branch, Technical Services &
483 Monitoring Division, Water Resources Services, Alberta Environmental Protection.

484

485 Celia, M.A., Bouloutas, E.T. and Zarba, R.L. (1990). A general mass-conservative
486 numerical solution for the unsaturated flow equation. *Water resources research*, **26**,
487 1483-1496. DOI: 10.1029/WR026i007p01483

488

489 Davies, G.M., Gray, A., Rein, G. and Legg, C.J. (2013). Peat consumption and carbon
490 loss due to smouldering wildfire in a temperate peatland. *Forest Ecology and*

491 *Management*, **308**, 169-177. DOI: 10.1016/j.foreco.2013.07.051

492
493 Devito, K.J., Mendoza, C., Qualizza, C. (2012). Conceptualizing water movement in the
494 Boreal Plains. Implications for watershed reconstruction. Synthesis report prepared for
495 the Canadian Oil Sands Network for Research and Development, Environmental and
496 Reclamation Research Group. 164p. DOI: 10.7939/R32J4H

497
498 Devito, K.J., Mendoza, C., Petrone, R.M., Kettridge, N. and Waddington, J.M. (2016).
499 Utikuma Region Study Area (URSA)–Part 1: Hydrogeological and ecohydrological
500 studies (HEAD). *The Forestry Chronicle*, **92**, 57-61. DOI: 10.1029/2007WR005950

501
502 Fenton, M.M., Waters, E.J., Pawley, S.M., Atkinson, N., Utting, D.J., McKay, K. (2013).
503 Surficial Geology of Alberta; Alberta Energy Regulator, AER/AGS Map 601, Scale 1:1
504 000 000.

505
506 Frandsen, W.H. (1998). Heat flow measurements from smoldering porous
507 fuel. *International Journal of Wildland Fire*, **8**, 137-145.

508
509 Hokanson, K.J., Lukenbach, M.C., Devito, K.J., Kettridge, N., Petrone, R.M. and
510 Waddington, J.M. (2016). Groundwater connectivity controls peat burn severity in the
511 boreal plains. *Ecohydrology*, **9**, 574-584. DOI: 10.1002/eco.1657

512
513 Lukenbach, M.C., Hokanson, K.J., Moore, P.A., Devito, K.J., Kettridge, N., Thompson,
514 D.K., Wotton, B.M., Petrone, R.M. and Waddington, J.M. (2015). Hydrological controls

on deep burning in a northern forested peatland. *Hydrological Processes*, **29**, 4114-4124.

DOI: 10.1002/hyp.10440

Lukenbach, M.C., Hokanson, K.J., Devito, K.J., Kettridge, N., Petrone, R.M., Mendoza, C.A., Granath, G. and Waddington, J.M. (2017). Post-fire ecohydrological conditions at peatland margins in different hydrogeological settings of the Boreal Plain. *Journal of Hydrology*, **548**, 741-753. DOI: 10.1016/j.jhydrol.2017.03.034

Moore, P.A., Morris, P.J. and Waddington, J.M. (2015). Multi-decadal water table manipulation alters peatland hydraulic structure and moisture retention. *Hydrological Processes*, **29**, 2970-2982. DOI: 10.1002/hyp.10416

Rein, G., Cleaver, N., Ashton, C., Pironi, P., Torero, J. (2008). The severity of smouldering peat fires and damage to the forest soil. *Catena*, **74**, 304-309. DOI: 10.1016/j.catena.2008.05.008.

Shaposhnikov, D., Revich, B., Bellander, T., Bedada, G. B., Bottai, M., Kharkova, T., Pershagen, G. (2014). Mortality related to air pollution with the Moscow heat wave and wildfire of 2010. *Epidemiology*, **25**(3), 359-364.

Siegel, D.I. (1988). The recharge-discharge function of wetlands near Juneau, Alaska: Part II. Geochemical investigations. *Groundwater*, **26**, 580-586.

Smerdon, B.D., Devito, K.J., Mendoza, C.A. (2005). Interaction of groundwater and

shallow lakes on outwash sediments in the sub-humid Boreal Plains of Canada. *Journal of Hydrology*, **314**, 246-262. DOI:10.1016/j.jhydrol.2005.04.001

Thompson, D.K. and Waddington, J.M. (2013). Peat properties and water retention in boreal forested peatlands subject to wildfire. *Water Resources Research*, **49**, 3651-3658. DOI: 10.1002/wrcr.20278

Thompson, D.K., Wotton, B.M. and Waddington, J.M. (2015). Estimating the heat transfer to an organic soil surface during crown fire. *International Journal of Wildland Fire*, **24**, 120-129. DOI: 10.1071/WF12121

Turetsky, M., Wieder, K., Halsey, L., Vitt, D. (2002). Current disturbance and the diminishing peatland carbon sink. *Geophysical Research Letters*, **29**, 21-1. DOI: 10.1029/2001GL014000.

Turetsky, M.R., Amiro, B.D., Bosch, E. and Bhatti, J.S. (2004). Historical burn area in western Canadian peatlands and its relationship to fire weather indices. *Global Biogeochemical Cycles*, **18** DOI: 10.1029/2004GB002222

von Post, L., Granlund, E. (1926). Peat resources in the south of Sweden. *Sveriges Geologiske Undersøkelser Serie CA*, **335**, 1–127.

Waddington, J.M., Morris, P.J., Kettridge, N., Granath, G., Thompson, D.K. and Moore, P.A. (2015). Hydrological feedbacks in northern peatlands. *Ecohydrology*, **8**, 113-127.

563 DOI: 10.1002/eco.1493

564

565 Yu, Z. (2011). Holocene carbon flux histories of the world's peatlands: Global carbon-
566 cycle implications. *The Holocene*, **21**, 761-774. DOI: 10.1177/0959683610386982

567

Table 1: Historical water-table depth (WTD) range and site characteristics at the flow through (Site FT), ephemerally perched (Site EP), and perched (Site P) peatlands in the URSA coarse-grained hydrological response area.

Variable	FT	EP	P
Peatland margin WTD (m)*			
Historic range	0.32 to 0.00	0.88 to 0.45	0.75 to -0.01
2013-2014 median	-0.04	0.72	2.82
2013-2014 quartiles	(-0.11, 0.05)	(0.52, 0.85)	(2.24, 3.32)
Peatland middle WTD (m)*			
Historic range	0.21 to -0.02	0.92 to 0.43	0.41 to 0.00
2013-2014 median	0.04	0.74	0.15
2013-2014 quartiles	(0,0.11)	(0.5, 0.89)	(0.05, 0.25)
Peatland area (ha)	0.79	0.68	1.56
Peatland perimeter (m)	709	707	906
Average margin width (m)	2	10	6
Margin area (ha)	0.04	0.23	0.26
Margin cover (%)	5.5	34.4	16.6
Average von Post	2.2	6.6	4.8
Hummock cover (%)	64	40	45

*long term WTD data collection part of long term URSA study (Devito *et al.*, 2016)

569 Table 2: Average bulk density (ρ_b ; kg m⁻³) profiles, with standard error of the mean in parentheses, at the flow through (Site FT),
 570 ephemerally perched (Site EP), and perched (Site P) peatlands in the URSA coarse-grained hydrological response area. Number of
 571 measurements denoted by n .
 572

	Site FT				Site EP				Site P			
	Margin		Middle		Margin		Middle		Margin		Middle	
Depth (m)	n	ρ_b	n	ρ_b	n	ρ_b	n	ρ_b	n	ρ_b	n	ρ_b
0.02	12	40 (7)	6	27 (4)	16	79 (5)	7	26 (6)	6	74 (8)	3	27 (2)
0.06	12	53 (9)	6	42 (10)	15	76 (6)	7	36 (4)	6	71 (7)	3	40 (6)
0.10	9	41 (8)	6	46 (11)	16	85 (8)	7	48 (7)	6	87 (9)	3	50 (6)
0.14	9	49 (5)	6	48 (9)	15	117 (8)	7	44 (4)	6	100 (14)	3	62 (10)
0.18	9	67 (9)	6	48 (13)	15	169 (20)	7	51 (13)	6	133 (17)	3	78 (10)
0.22	6	70 (16)	6	57 (10)	14	156 (25)	7	80 (23)	6	147 (18)	3	90 (6)
0.26	3	112 (39)	4	61 (21)	13	176 (19)	7	103 (19)	5	130 (5)	3	94 (8)
0.30	2	221 (48)	4	64 (19)	13	217 (20)	7	129 (23)	5	146 (6)	3	110 (8)
0.34	1	231 (--)	4	75 (29)	12	252 (20)	7	150 (21)	5	165 (8)	3	107 (2)
0.38	1	289 (--)	3	76 (28)	11	272 (34)	7	172 (24)	5	167 (7)	3	112 (1)
0.42			4	92 (42)	9	240 (23)	7	199 (32)	4	169 (18)	3	105 (5)
0.46					9	277 (43)	4	295 (24)	4	182 (32)	3	115 (2)
0.50					6	343 (56)	3	299 (30)	2	297 (46)	1	130 (--)
0.54					1	301 (--)						

Table 3: ANOVA results for simulated volumetric water content (VWC), and H_{comb}/H_{ign} ratios

	Factor	Sum of Square	d.f.	F-stat	p-value
VWC	Depth	2.43	1	114.9	4.7E-19
	Site	4.86	2	114.7	3.3E-28
	WT Scenario	0.21	1	9.7	2.2E-03
	Location (middle v. margin)	0.21	1	9.8	2.2E-03
	Depth • Site	0.58	2	13.7	4.7E-06
	Depth • WT Scenario	0.03	1	1.4	0.25
	Depth • Location	0.36	1	17.1	6.9E-05
	Site • WT Scenario	0.07	2	1.7	0.18
	Site • Location	1.65	2	38.9	1.2E-13
	WT Scenario • Location	0.09	1	4.3	0.04
	Depth • Site • WT Scenario	0.06	2	1.5	0.23
	Depth • Site • Location	0.38	2	9.1	2.2E-04
	Depth • WT Scenario • Location	0.05	1	2.5	0.12
	Site • WT Scenario • Location	0.09	2	2.1	0.13
	Depth • Site • WT Scenario • Location	0.04	2	1.1	0.35
	<i>Factor = Error / Sum Sq = 2.46 / d.f. = 116</i>				
H_{comb}/H_{ign}	Depth	10.60	1	197.4	2.2E-26
	Site	29.98	2	279.2	4.7E-44
	WT Scenario	1.07	1	19.9	2.0E-05
	Location (middle v. margin)	9.81	1	182.8	3.3E-25
	Depth • Site	4.57	2	42.6	1.9E-14
	Depth • WT Scenario	0.03	1	0.51	0.47
	Depth • Location	2.58	1	48.1	2.9E-10
	Site • WT Scenario	0.15	2	1.4	0.26
	Site • Location	5.31	2	49.5	4.3E-16
	WT Scenario • Location	0.18	1	3.3	0.07
	Depth • Site • WT Scenario.	0.29	2	2.7	0.07
	Depth • Site • Location	1.64	2	15.2	1.4E-06
	Depth • WT • Location	0.10	1	1.8	0.18
	Site • WT Scenario • Location	0.10	2	0.9	0.42
	Depth • Site • WT Scenario • Location	0.16	2	1.5	0.24
	<i>Factor = Error / Sum Sq = 5.96 / d.f. = 111</i>				

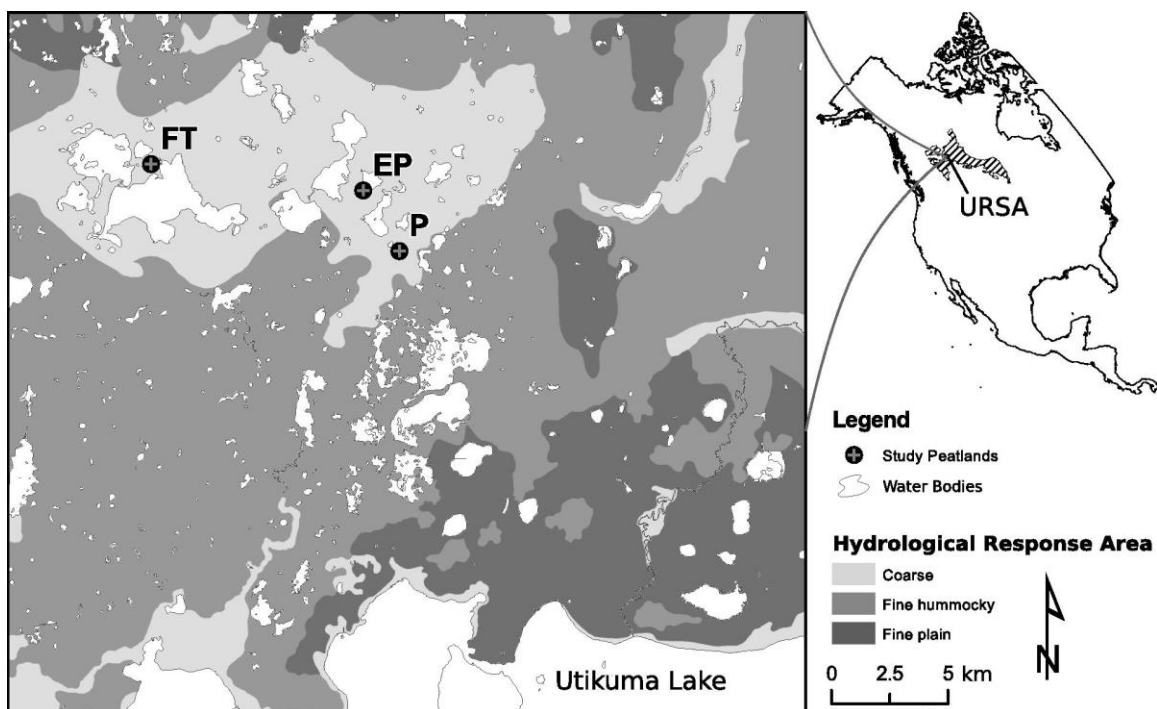


Figure 1: Location of flow-through (Site FT), ephemerally perched (Site EP) and perched (Site P) peatlands, and hydrography relative to the geology in the URSA (adapted from Fenton et al., 2013). Inset shows the URSA's relative position in the Boreal Plains and North America.

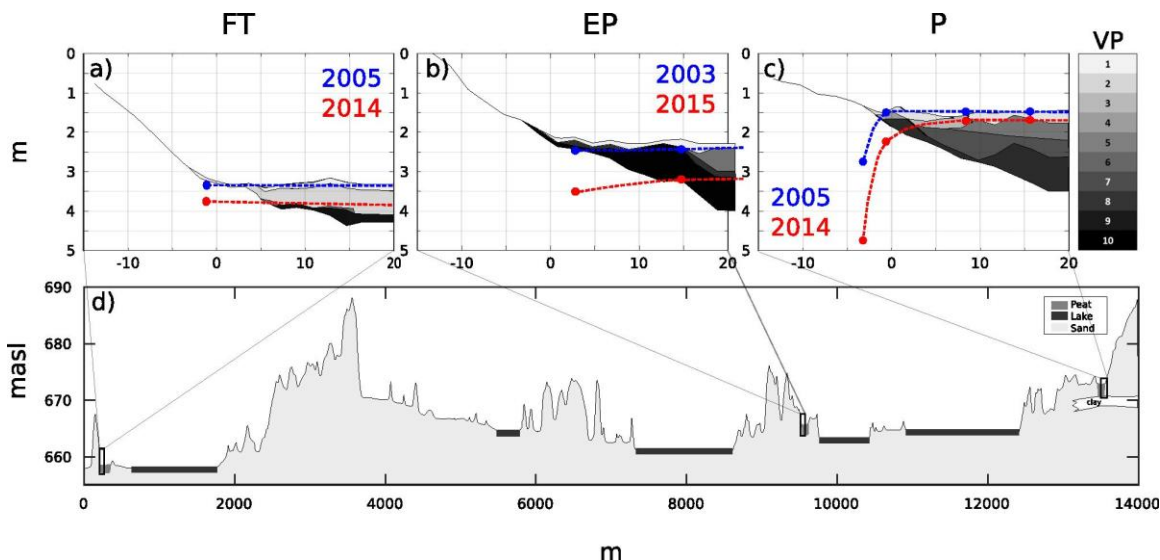
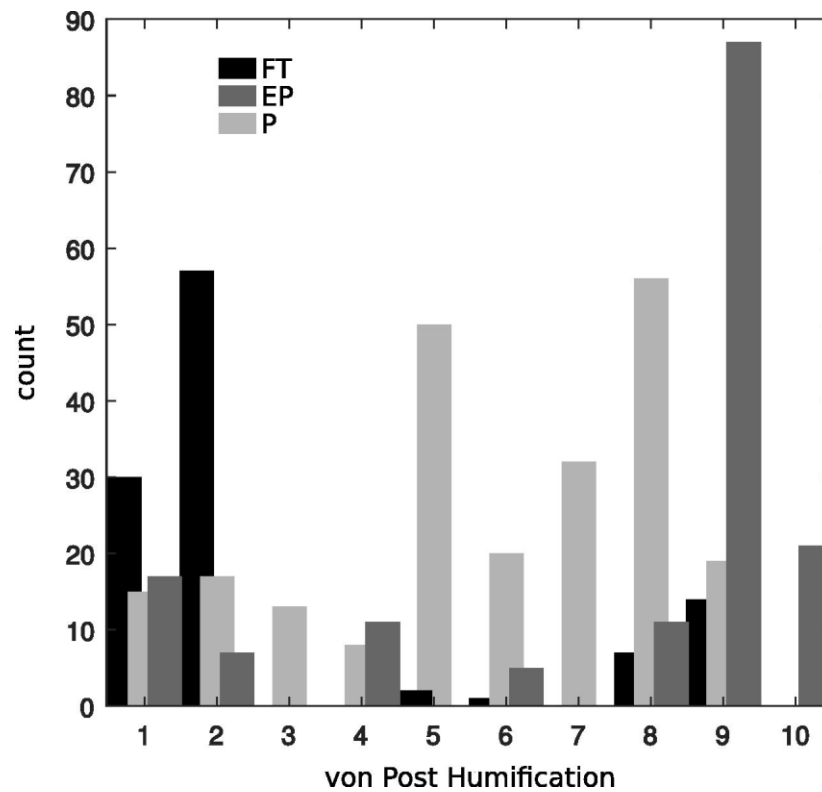


Figure 2: Cross section profiles along 20 m transects at the margins of (a) Site FT, (b) Site EP and (c) Site P. Historic high (blue) and low (red) water-table configurations are shown for each site. von Post depth-profiles (numerical scalebar) are also shown for each site. A cross section of the coarse textured outwash at the URSA (d) shows the relative topographic position of each site. Vertical exaggeration is ~2.5 times.



586

587 Figure 3: Histogram of von Post humification indices observed at site FT, EP, and P. Each
 588 count represents a cored sample from the 20 m transect, where VP samples were taken
 589 every 0.05m vertically and 1m horizontally.

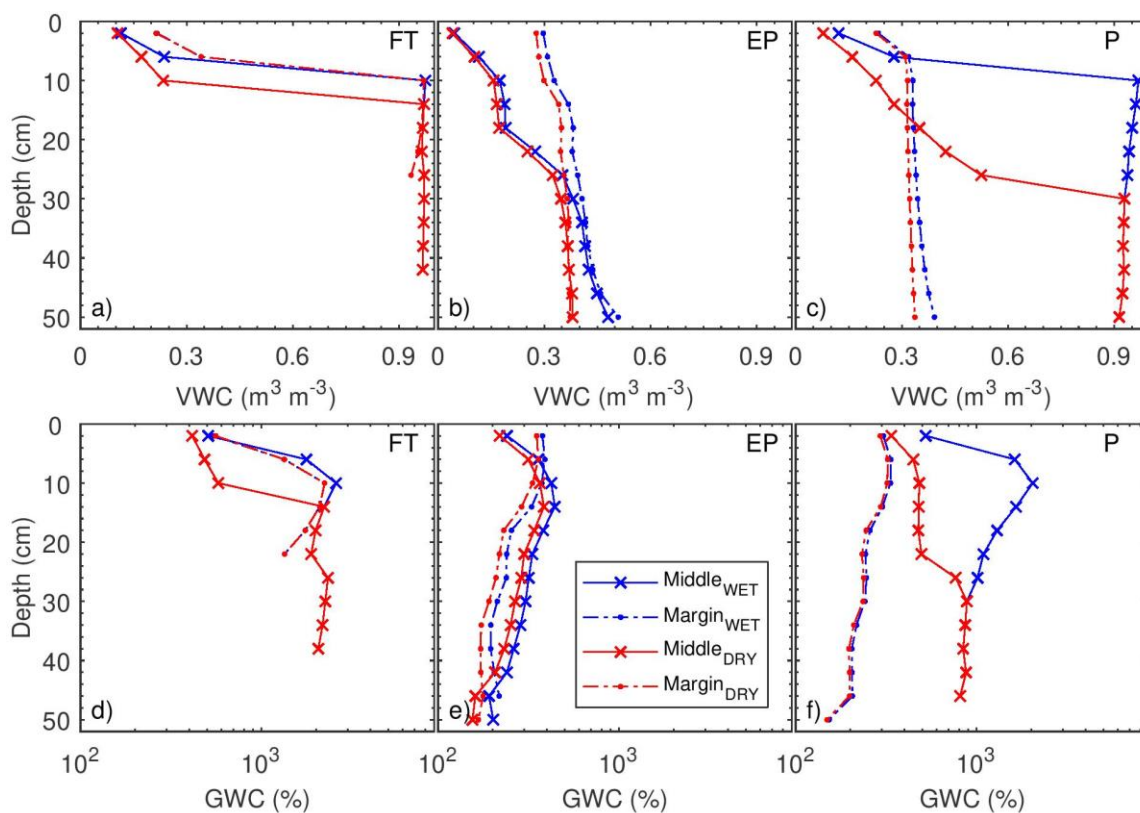


Figure 4: Simulated volumetric water content (a-c) and gravimetric water content (d-f) for middle (solid line with 'x' marker) and margin (dashed line with dot marker) locations at three peatlands (FT, EP, and P sites) in a coarse-grained hydrological response area

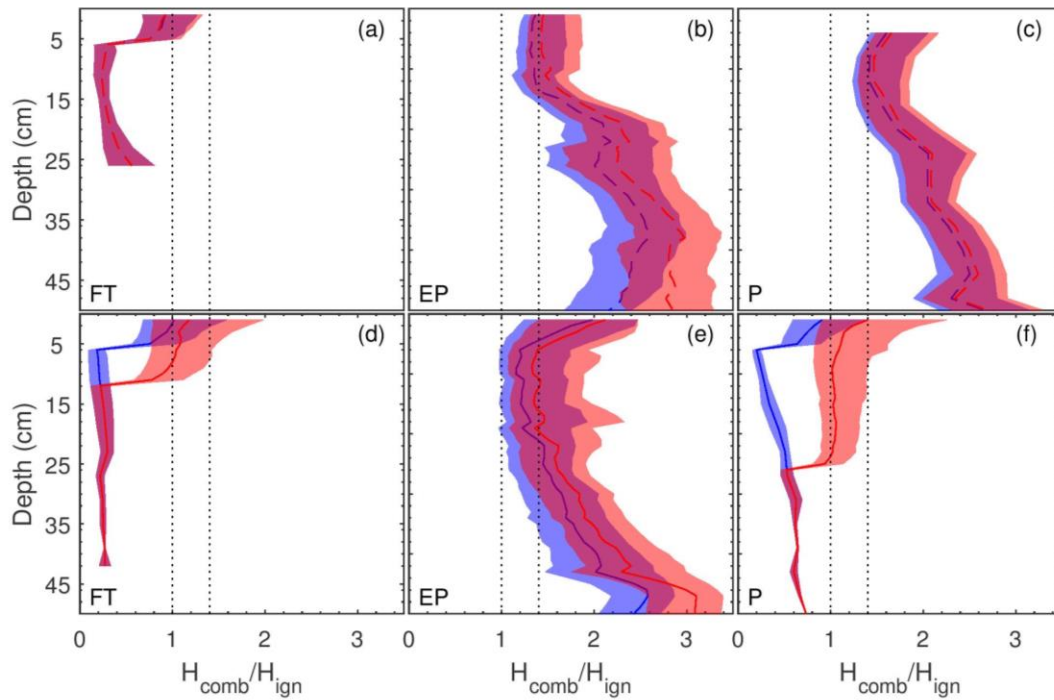


Figure 5: Simulated ratio for heat of combustion over heat of ignition (H_{comb}/H_{ign}) for margin (a-c) and middle (d-f) locations. Red and blue lines indicate the median simulated H_{comb}/H_{ign} ratio for dry and wet WT scenarios, respectively. Shaded areas represent the range in simulated data from the 5th to 95th percentile. Dotted vertical lines at 1.0 and 1.4 indicate the ratio of heat of combustion to heat of ignition required to sustain smouldering at downward heat efficiencies of 1.0 and 0.7, respectively.

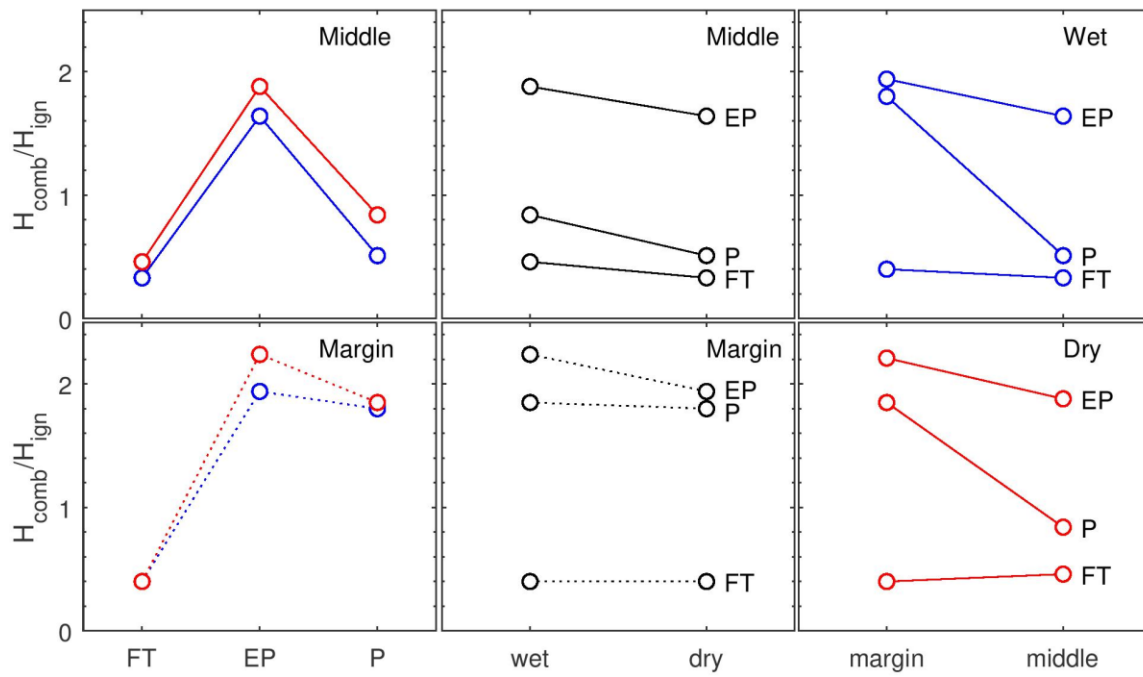


Figure 6: Interaction plot for general linear model of H_{comb}/H_{ign} showing all two-way interactions between site (FT, EP, P), WT scenarios (wet and dry) and location (margin and middle). Comparison of top and bottom panels are meant to show three-way interactions.